Journal of Innovation and Development
ISSN: 2958-4752 | Vol. 9, No. 3, 2024

Optimal Design of Cleaning Performance for Tobacco Residues Self-Cleaning Robots

Kai Zhao[1], Buyun Xu[2], Guisen Wang[2], Huli Niu[2] and Haipeng Yan[2,*]

[1]Department of Hebei Baisha Tobacco Company, Shijiazhuang 052165, China
[2]School of Mechanical Engineering, Hebei University of Science and Technology, Shijiazhuang 050018, China
[*]Corresponding author: lnyanhp@126.com

Abstract: In response to the challenges presented by the strong adhesion of tobacco dregs and the difficulties in cleaning, an intelligent self-cleaning robot has been devised and developed for the complex environment at the bottom of distribution vehicles. By integrating a scraping mechanism, a sweeping system, and a vacuuming device, an efficient and collaborative cleaning solution has been established to effectively meet the requirements for cleaning and absorbing tobacco residue. Kinematic and rigid body dynamics analyses have been carried out on the key tobacco scraper device to optimize its motion trajectory and evaluate its mechanical response, thereby guaranteeing high efficiency and stability during the cleaning process. Test results show that this mechanism can precisely scrape and collect the tobacco residue, avoiding excessive friction and cleaning blind spots. It can converge scattered tobacco dregs to cover more than 20% of the area. The intelligent self-cleaning robot proposed in this study demonstrates outstanding performance in handling tobacco residue cleaning issues, meeting the high demands for cleaning efficiency and quality within the tobacco industry, and has significant application value and development prospects.

Keywords: Tobacco residue; scraper mechanism; kinematic analysis; rigid body dynamics analysis; cleaning efficiency; mechanical response.

1. Introduction

According to statistics from the World Health Organization (WHO), approximately one billion people worldwide use cigarettes, with an annual production of over 2.5 million tons of tobacco in China alone, accounting for about half of global production. Due to its large output and high economic benefits, effective pest control measures are crucial for ensuring both economic viability in the tobacco industry and food safety. One primary source of pests arises from tobacco dregs that falls throughout production lines during transportation and is not cleaned promptly, along with residual insect eggs from harvesting processes. Moreover, the dimly lit and confined space at the bottom of tobacco distribution vehicles complicates cleaning efforts, making it a main source of pests. Pest excrement and carcasses are major contributors to mold growth on tobacco products, while live pests can damage both tobacco leaves and cigarette paper, leading to defects in finished products as illustrated in Figure 1, which will also affect the smoking taste of cigarettes during sensory evaluation. According to the survey data, the tobacco storage loss caused by tobacco bugs has reached about 250 million yuan, of which the direct cigarette loss rate caused by tobacco bugs is about 0.716%, and there is no effective solution to this problem.

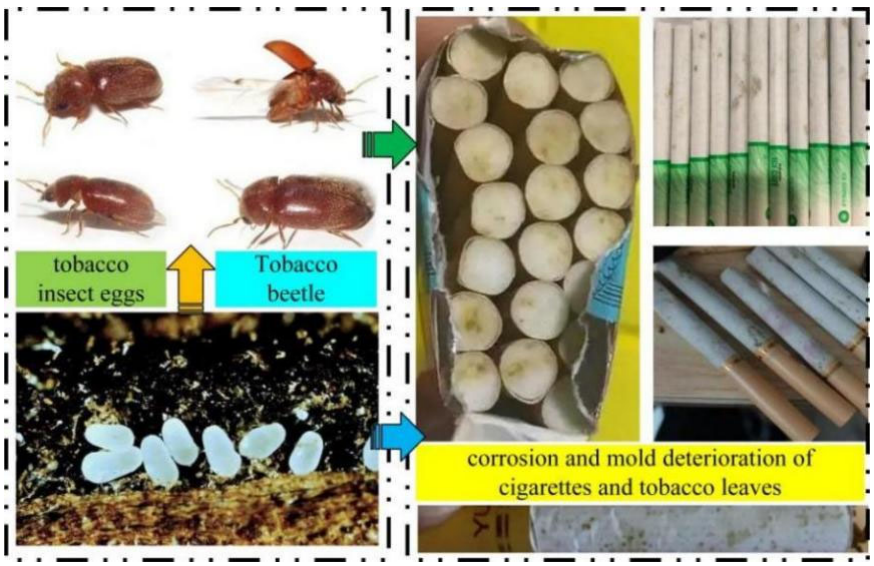


Figure 1. Overview of breeding of Tobacco Insect and Corrosion in cigarette

Currently, both domestic and international efforts to address the problem of tobacco dust focus primarily on

cleanliness and leakage prevention. In terms of leakage prevention, Shuhao Zhang. designed a specialized brush structure based on the structural characteristics of tobacco residue to intercept it at its source [1]. As for cleaning tobacco residue, various cleaning robots have played a major role. For instance, Donghun Lee et al. combined a seven-axis redundant robotic arm with a six-degree-of-freedom RRX mobile platform to develop an automated cleaning robot system [2]. Maryam Kouzehgar et al. proposed a modular cleaning robot named Mantis that employs a convolutional neural network (CNN) based deep learning detection system [3]. Jonghoek Kim introduced an autonomous sweeping system composed of small cleaning robots (CR) and large dust storage robots (SR) aimed at overcoming traditional robots' limitations regarding cleaning capacity and their inability to access narrow spaces [4]. T. Palleja developed a cleaning robot based on a vision measurement system capable of real-time recording and analyzing cleaning trajectories and coverage areas [5].

However, the bottom of distribution vehicles is relatively dimly lit and confined, situated approximately four meters above ground level as shown in Figure 2. Additionally, accumulated tobacco residue on the bottom tray can lead to sediment buildup that obstructs material flow, causing moist and greasy tobacco residues to adhere extensively to tray surfaces. Consequently, existing cleaning solutions are challenging to implement in this environment and fail to resolve these technical difficulties. Therefore, in view of the above technical difficulties and the complexity of the working condition, an intelligent self-cleaning robot has been designed that effectively removes adhesive tobacco residues. Through kinematic analysis and rigid body dynamics analysis of the scraper mechanism located at the front side of the robot body, its scraping trajectory and performance have been optimized while verifying structural stability. Furthermore, fluid simulation data from vacuum fans have been utilized to evaluate overall cleaning effectiveness.

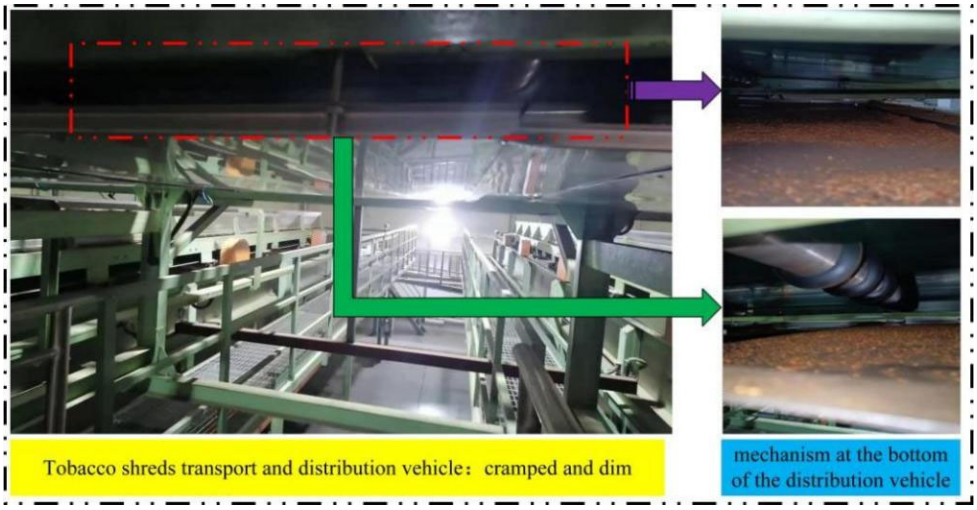


Figure 2. Complex condition of the bottom of distribution vehicles

2. Design and Principle Analysis of the Cleaning Robot Mechanism

The main structure of the cleaning robot is illustrated in Figure 3. The use of a Mecanum-wheel mobile robot (MWMR), known for its omnidirectional mobility and excellent stability and maneuverability, has led to its widespread application across various fields [6]. This design incorporates a reduction drive structure centered around the Mecanum wheel, enabling the robot to perform omnidirectional movements. This capability allows it to navigate effectively on uneven surfaces while executing comprehensive cleaning tasks without leaving any blind spots. The design of the Mecanum wheel permits multiple modes of motion—including forward, backward, lateral, and diagonal movements—without altering the direction of travel, thereby facilitating efficient operation even in confined spaces. Additionally, the robot is equipped with a high-efficiency vacuum fan and a tobacco residue collection box at its base. Through negative pressure, this system effectively draws in tobacco residue and dust into the collection box, ensuring that debris generated during the cleaning process is efficiently captured. To further enhance cleaning efficiency, an electric sweeping system is installed at the front of the robot. This system utilizes rotating bristles to gather tobacco residue and debris toward the fan's inlet, thereby achieving a synergistic effect between sweeping and vacuuming.

Moreover, the robot features a scraper mechanism based on a linkage-slider mechanism designed to gather scattered tobacco residue from the ground into the sweeping area. The linkage-slider mechanism facilitates linear reciprocating motion of the gathering rod through efficient mechanical transmission. As the gathering rod moves forward, it effectively scrapes up tobacco residue and concentrates it in the sweeping area before directing it toward the fan inlet. This gathering function works in tandem with both the sweeping and vacuum systems to ensure that tobacco residue and dust are rapidly cleared and effectively drawn into the collection box, thus preventing secondary dispersal. The structural design of this robot optimizes its movement system, cleaning devices, and gathering mechanism to create an efficient collaborative cleaning solution that not only achieves effective collection and clearance of tobacco residue but also ensures high performance and stability throughout the cleaning process.

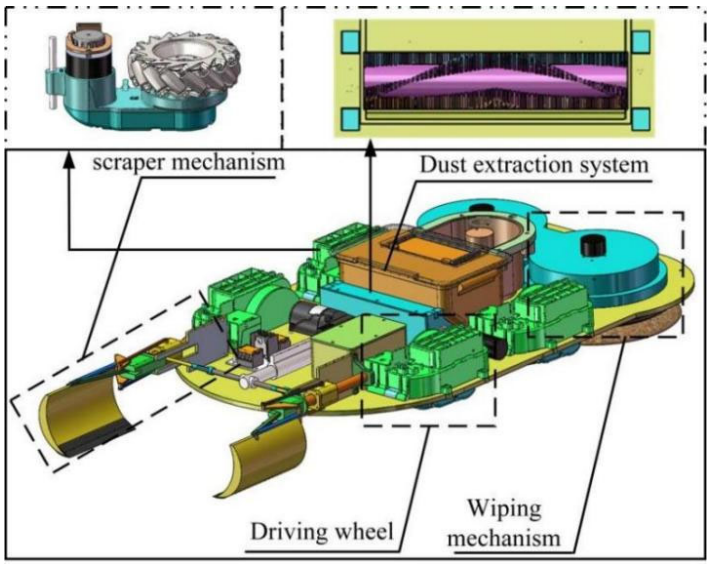


Figure 3. Main structure overview of Tobacco residues Self-Cleaning Robots

3. Research Design of Scraping Mechanism Based on Tobacco Characteristics

Tobacco contains certain oils and moisture that can cause its surface to become slippery under high-temperature or humid conditions. During transportation, as tobacco accumulates, strong adhesion develops between oil-water molecules and conveyor belt surfaces, leading to tobacco sticking to belts. Additionally, the fine particles and fibrous structure of tobacco increase its contact area with belt surfaces, exacerbating adhesion issues. This phenomenon is particularly pronounced on conveyor belts with high friction coefficients. Based on tobacco characteristics and structure, a scraper mechanism has been designed and developed as shown in Figure 4. This device aims to effectively scrape off tobacco residue adhering to tray surfaces while facilitating collection to work in conjunction with sweeping brushes and fans for collection, absorption, and storage processing.

This mechanism primarily relies on reciprocating gathering motion. The four-bar linkage mechanism consists of rigid links designed for path generation or functional movement [7], leading to an overall design optimized based on a crank-rocker mechanism. Furthermore, since the crank-slider mechanism evolved from crank-link mechanisms—characterized by simplicity in structure, smooth motion, and high transmission efficiency—it finds extensive applications in equipment such as presses, internal combustion engines, conveyors, and reciprocating pumps. Consequently, the driving device (electric push rod) can effectively transmit power through the crank-slider mechanism to drive end-effector gathering actions. Thus, building upon a crank-rocker foundation while integrating stable transmission characteristics from crank-sliders has led to an optimized design for the primary driving mechanism of the scraping device (i.e., crank-rocker-slider mechanism).

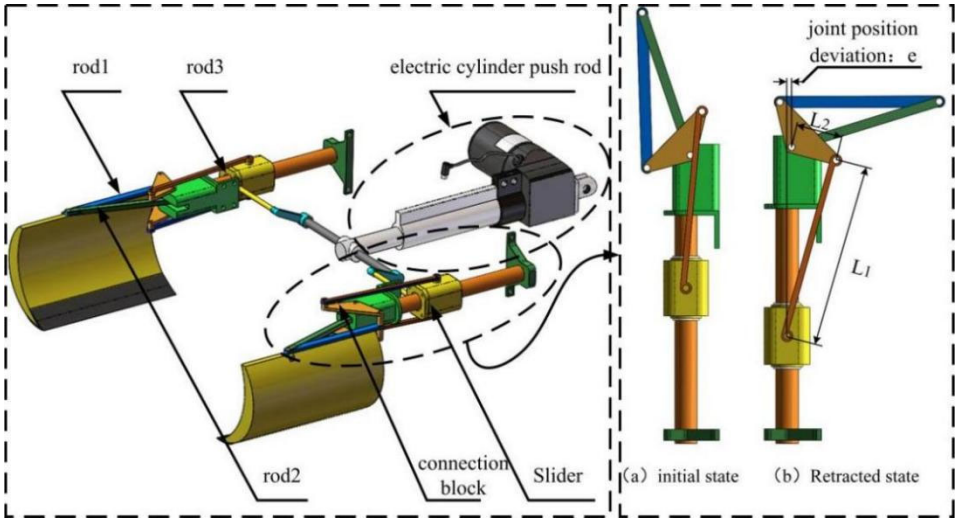


Figure 4. Structure overview of scraper device

3.1. Study on the end-effector pose trajectory of the folding mechanism based on kinematic analysis

The classic path generation problem in four-bar mechanisms involves determining the linkage parameters such that a specified point on the coupler follows a predetermined trajectory [9-10]. Consequently, kinematic equations for the scraper device's motion are established, and a "cloud map" of its end-effector pose trajectory is generated.

Through an analysis of its motion states, the optimal scraping path is refined to enhance cleaning effectiveness. Precise pose design ensures that the scraper covers all cleaning areas, thereby avoiding omissions or excessive friction, which improves both uniformity and efficiency in cleaning. The optimized kinematic model reduces unnecessary redundant movements, lowers energy consumption and mechanical wear, while ensuring high efficiency and stability during the cleaning process, ultimately enhancing the overall performance and durability of the robots.

The Denavit-Hartenberg (D-H) parameter method can be employed to model jointed serial structures and to derive transformation matrices from the center of mass to the end effector [8]. To solve the kinematic equations for the folding mechanism, we take the fixed end O_0 coordinate system as the origin and determine the corresponding position coordinates for each joint through positional transformations. This coordinate transformation can be described using vectors and rotation matrices. In this scraper mechanism, we establish a reference coordinate system at O_0-$X_0Y_0Z_0$, where the X-Y axes represent translational motion directions and the Z-axis serves as the rotational reference axis for each joint. The D-H coordinate system is created as illustrated in Figure 5, with specific steps for coordinate transformation outlined as follows:

To determine the relative positions of each joint's coordinate system within the D-H coordinate system, we proceed as follows: First, translate the O_0-$X_0Y_0Z_0$ coordinate system along the X direction by L_1 to reach point O_1. Next, rotate around Z_1 by an angle θ_1 and then translate by L_2 to point O_2. Subsequently, rotate around Z_2 by θ_2 and translate by L_3 to point L_3. Finally, rotate around Z_3 by θ_3 and translate by L_4 to reach point O_4, which represents the end position of execution.

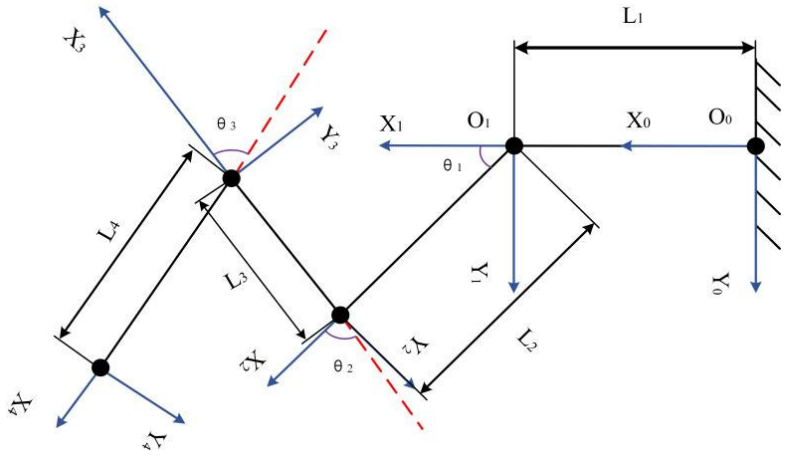


Figure 5. D-H coordinate system of transmission device

The solving process of above coordinate system is represented in expressions (1) - (4).

$$A_1^0 = trans\begin{pmatrix} L_1 & 0 & 0 \end{pmatrix}$$

$$A_1^0 = \begin{bmatrix} 1 & 0 & 0 & L_1 \\ 0 & 1 & 0 & 0 \\ 0 & 0 & 1 & 0 \\ 0 & 0 & 0 & 1 \end{bmatrix} \tag{1}$$

$$A_2^1 = Rot\begin{pmatrix} Z_1 & \theta_1 \end{pmatrix} \bullet Trans\begin{pmatrix} L_2 & 0 & 0 \end{pmatrix}$$

$$A_2^1 = \begin{bmatrix} \cos\theta_1 & \sin\theta_2 & 0 & L_2\cos\theta_1 \\ \sin\theta_1 & \cos\theta_1 & 0 & L_2\sin\theta_1 \\ 0 & 0 & 1 & 0 \\ 0 & 0 & 0 & 1 \end{bmatrix} \tag{2}$$

$$A_3^2 = Rot\begin{pmatrix} Z_2 & \theta_2 \end{pmatrix} \cdot Trans\begin{pmatrix} L_3 & 0 & 0 \end{pmatrix}$$

$$A_3^2 = \begin{bmatrix} \cos\theta_2 & -\sin\theta_2 & 0 & L_3\cos\theta_2 \\ \sin\theta_2 & \cos\theta_2 & 0 & L_3\sin\theta_2 \\ 0 & 0 & 1 & 0 \\ 0 & 0 & 0 & 1 \end{bmatrix} \tag{3}$$

$$A_4^3 = Rot\begin{pmatrix} Z_3 & \theta_3 \end{pmatrix} \bullet Trans\begin{pmatrix} L_4 & 0 & 0 \end{pmatrix}$$

$$A_4^3 = \begin{bmatrix} \cos\theta_3 & -\sin\theta_3 & 0 & L_4\cos\theta_3 \\ \sin\theta_3 & \cos\theta_3 & 0 & L_4\sin\theta_3 \\ 0 & 0 & 1 & 0 \\ 0 & 0 & 0 & 1 \end{bmatrix} \tag{4}$$

$$T_4 = A_1^0 \cdot A_2^1 \cdot A_3^2 \cdot A_4^3$$

$$= \begin{bmatrix} \cos\theta_1\cos\theta_2\cos\theta_3 & -\sin\theta_1\sin\theta_2\sin\theta_3 & 0 & L_3\cos\theta_1\cos\theta_2\cos\theta_3 + L_2\cos\theta_1\cos\theta_2 + L_4\cos\theta_1 + 68 \\ \sin\theta_1\sin\theta_2\sin\theta_3 & \cos\theta_1\cos\theta_2\cos\theta_3 & 0 & L_3\sin\theta_1\sin\theta_2\sin\theta_3 + L_2\sin\theta_1\sin\theta_2 + L_4\sin\theta_1 \\ 0 & 0 & 1 & 0 \\ 0 & 0 & 0 & 1 \end{bmatrix} \tag{5}$$

The expression results for solving the kinematic equations of the scraper mechanism are provided in expression (5). Using MATLAB based on these kinematic equations, we plot a "cloud map" of its end effector's spatial trajectory as shown in Figure 6 (unit: mm). As illustrated, the spatial trajectory of scraper fixed rod 1 takes on an arc shape with a covered area (i.e., cleaning area) of approximately 0.01 m², meeting expected cleaning specifications. Furthermore, analysis reveals that during the folding process of this mechanism, an appropriate distance between the two scrapers is maintained to prevent collisions effectively, thereby significantly reducing risks associated with jamming or system failures.

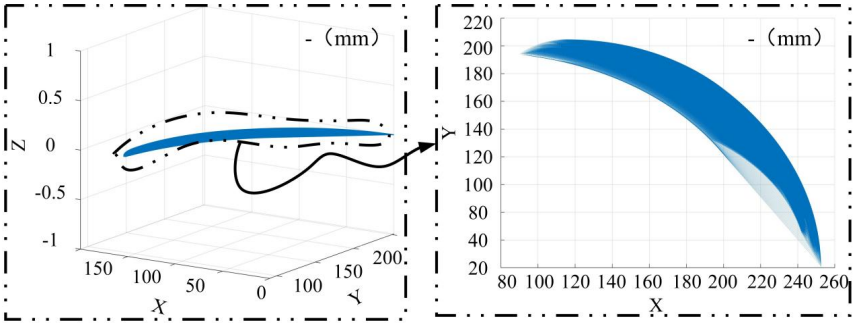


Figure 6. "Cloud Map" of the Motion Space of the scraper mechanism

3.2. Analysis of the Motion Characteristics and Mechanical Response of the Scraper Mechanism Based on Rigid Body Dynamics

During high-speed operation, flexible mechanism systems exhibit significant elastic vibration deflections, which can compromise motion accuracy and reduce the system's lifespan [11]. To evaluate the stability and reliability of the scraper mechanism, we conducted a rigid body dynamics simulation analysis on its key components. This study focuses on analyzing parameters such as displacement, velocity, acceleration, and angular displacement under specific motion patterns. The goal is to ensure that these parameters remain within prescribed fluctuation ranges for stable system operation while identifying potential dynamic hazards, such as fluctuations in operation and increases in internal friction, thereby enhancing system safety and reliability.

The simulation results for the rigid body kinematics of the scraper mechanism, along with the variation curves of key dynamic parameters such as displacement, velocity, and acceleration, are presented in Figure 7. As illustrated, the velocity begins to increase with the initiation of the folding action. Between 1.5 seconds and 5 seconds, the acceleration trend is relatively gentle, indicating a decrease in acceleration during this interval and a stable velocity change consistent with the characteristics of crank-rocker motion. Furthermore, this characteristic of acceleration variation and its fluctuation range effectively mitigate the risk of severe vibrations and high-impact loads that could compromise motion stability and contact uniformity, ultimately affecting cleaning quality. After accelerating for 0.7 seconds, the speed (V) reaches a peak value of 1.18 m/s. This speed variation characteristic and its fluctuation range ensure effective removal of adhering tobacco residue while avoiding excessive energy consumption and mechanical wear within the system due to high-speed operation.

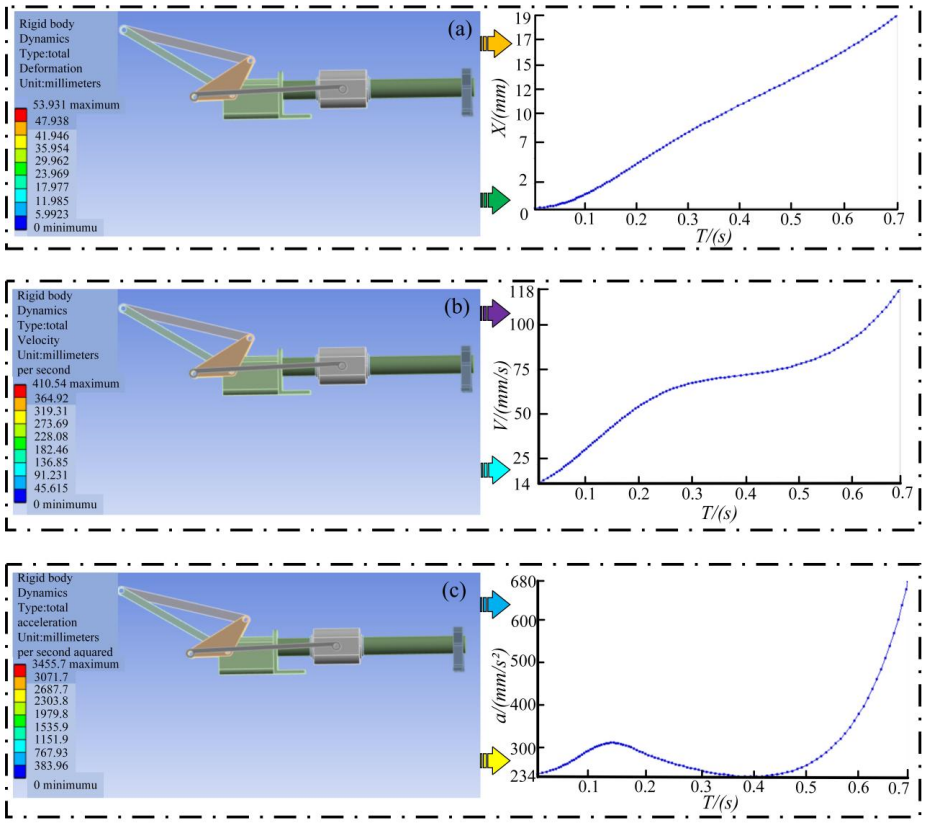


Figure 7. Dynamic simulation results and parameter variation curves of rigid body of scraper mechanism
(a) The results of rigid body dynamics deformation simulation and the variation curves;
(b) The results of rigid body dynamics velocity simulation and the variation curves;
(c) The results of rigid body dynamics acceleration simulation and the variation curves.

3.3. Functional Testing of the Scraper Mechanism

To further validate the operational effectiveness and mechanical response characteristics of the scraper mechanism, we assessed its scraping performance using components fabricated from 3D printing materials (such as PLA and TPU) that possess excellent flexibility, wear resistance, and comply with food-grade standards. The customized nature, lightweight design, and high precision afforded by 3D printing technology ensured that the structure and functionality of the scraper mechanism met practical application requirements. The testing materials utilized were made from steel plates identical to those used in the distribution vehicle chassis. The testing results are depicted in Figure 8. The scraper mechanism demonstrated efficient removal and aggregation of surface tobacco residue while operating stably; these findings align closely with both kinematic analysis results and rigid body dynamics simulation outcomes. The mechanical design of the mechanism is rationally conceived; it requires minimal force input and can utilize small drive devices suitable for confined spaces, significantly enhancing cleaning efficacy.

Additionally, through multiple tests involving scraping actions to assess aggregation effectiveness, we selected nine trials for comparative analysis; these results are shown in Figure 9. The data represent the area distribution of tobacco residue after aggregation compared to its distribution area prior to aggregation. The results indicate effective aggregation performance with an aggregated area exceeding 20%, which can even reach over 30% depending on variations in tobacco residue distribution.

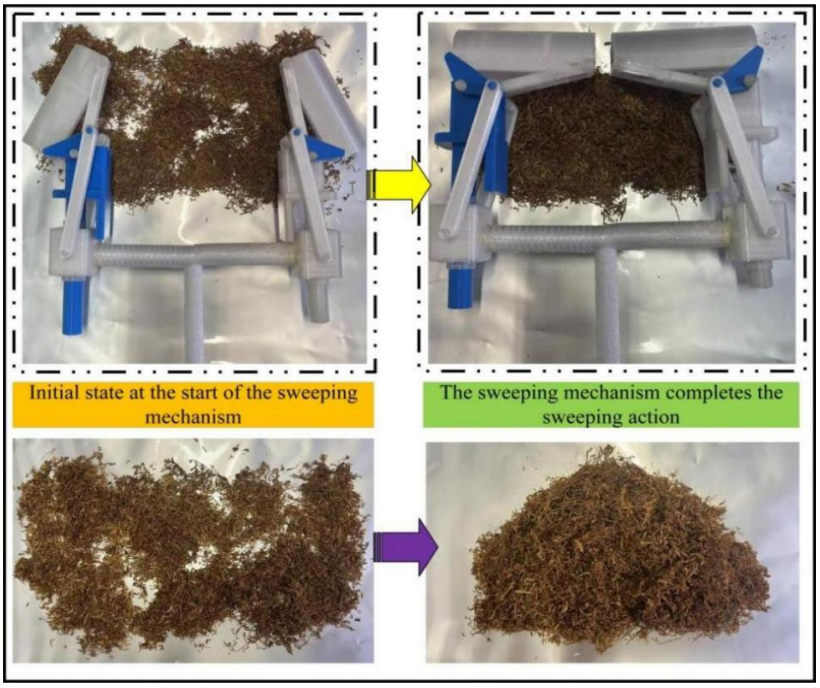


Figure 8. Diagram of scraper mechanism test

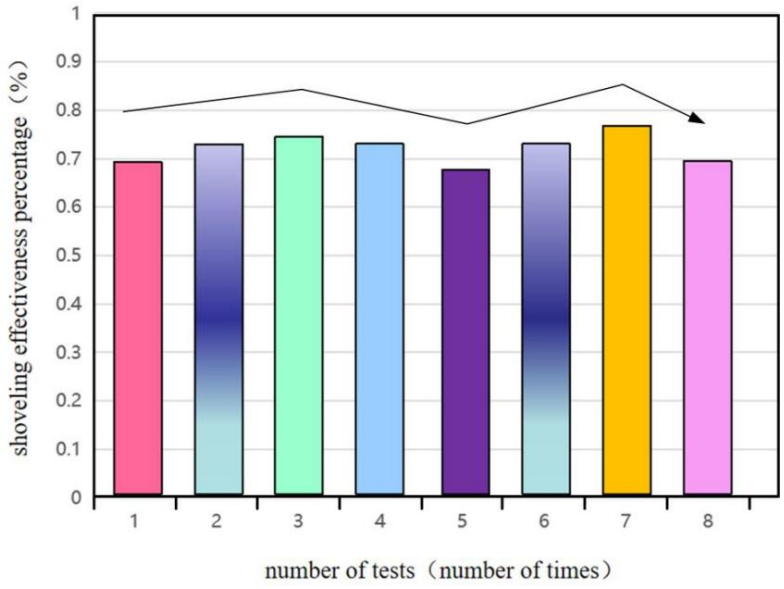


Figure 9. Results of tobacco residue distribution and gathering area ratio of scraper mechanism

4. Evaluation of Dust Collection Device Absorption Effect Based on Fluid Simulation Analysis

The dust collection device is a critical component for the robot's ability to perform tobacco residue cleaning, and its dust collection performance significantly impacts the overall cleaning efficacy of the robot. The main structure of this device is composed of essential components such as a fan and a filter element, all integrated within the collection box. Its operational principle primarily relies on the negative pressure effect generated by a centrifugal fan, which quickly draws airborne particulates into the dust collection box through airflow. Inside the dust collection box, an increase in cross-sectional area leads to a reduction in airflow velocity, resulting in the conversion of dynamic pressure into static pressure. This process decreases the force acting on dust particles in the horizontal direction, allowing them to gradually settle at the bottom of the collection box under the influence of gravity. However, smaller particles may not settle promptly; instead, they can be carried into the filter area by the airflow, where they are effectively filtered out by the filter element, thereby achieving efficient dust collection [12-13]. To verify whether its absorption effect meets expected cleaning requirements, fluid simulation of the airflow field around this dust collection fan was conducted. This was complemented by numerical analysis to assess static pressure fluctuations and evaluate cleaning performance, with relevant parameters presented in Table 1.

Table 1. Related parameters of dust collection mechanism

Diameter of Turbine	Hight of Turbine	Angular velocity of stable operating	Distance between inlet and fan	Boundary setting
88mm	35mm	50rad/S	150mm	170mm

The results of the fluid simulation are illustrated in Figure 10. The wind speed at the boundary before the fan outlet can reach 0.13 m/s. Although this wind speed is relatively low, it is sufficient to generate stable negative pressure in this region, ensuring that tobacco residue is drawn in without causing reverse lifting or suspension phenomena. An appropriate wind speed helps maintain airflow stability, preventing instability and lifting of tobacco residue that can occur with excessively high speeds. At this point, the static pressure inside the collection box exceeds 1 MPa, providing ample energy to overcome particle inertia, frictional forces, and adhesion to surfaces or other objects. This ensures that even small or lightweight tobacco residues can be swiftly dislodged from surfaces and drawn into the system.

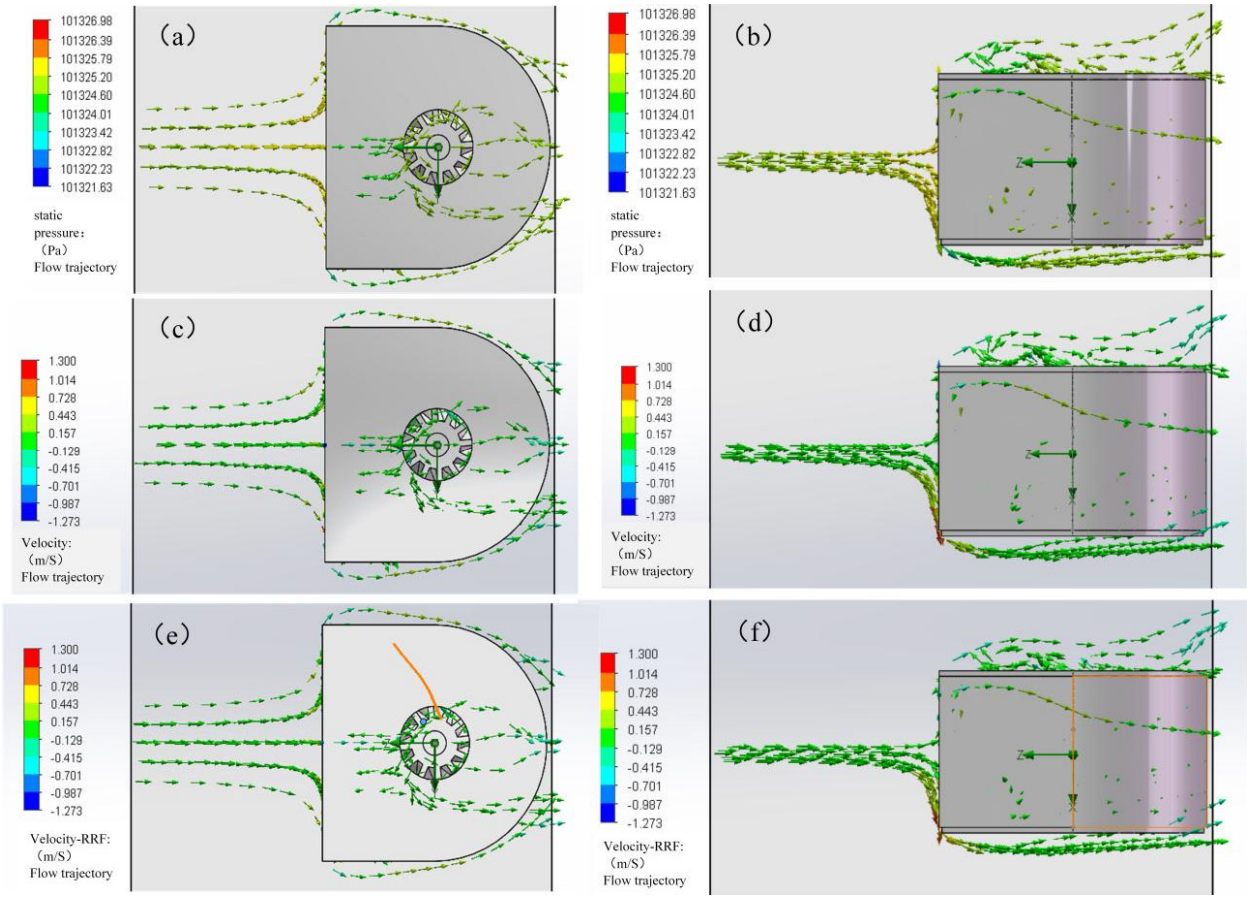


Figure 10. Simulation results of wind speed hydrostatic fluid of dust collection mechanism
(a) and (b)- Static pressure of dust collection mechanism;
(c) and (d)-Velocity of dust collection mechanism;
(e) and (f)-Response speed of dust collection mechanism.

5. Conclusion

By establishing kinematic equations for scraper mechanism of the cleaning robot and mapping its operational trajectory, we conducted finite element analysis using rigid body dynamics on this scraper mechanism alongside experimental tests for its scraping capabilities. The results from these analyses demonstrate that this robot effectively addresses issues related to tobacco residue adhesion. Additionally, fluid simulation results for the dust collection mechanism indicate that its cleaning system performs well in removing tobacco residues, showcasing good synergy between both components. The design and development of this intelligent self-cleaning robot provide an innovative solution for cleaning and maintenance during cigarette manufacturing processes, offering significant practical value by effectively mitigating issues related to tobacco residue accumulation that can lead to pest breed and subsequent economic losses within the tobacco industry.

Acknowledgements

The authors gratefully acknowledge the financial support from Research and Practice Project on Innovation and Entrepreneurship Education Teaching Reform in Higher Education Institutions in Hebei Province (2023cxcy088) and Collaborative Education Project of Industry University Research by the Ministry of Education (2410314936 and 2412030712).

References

[1] Zhang S, Cao X, Xue W, et al. Preparation, characterization, and synergistic soil moisture retention effects of a by-product-based dust suppressant for fugitive dust suppression. Atmospheric Pollution Research, 2024, 15(3): 102004.

[2] Lee D, Ku N, Kim T W, et al. Self-traveling robotic system for autonomous abrasive blast cleaning in double-hulled structures of ships. Automation in Construction, 2010, 19(8): 1076-1086.

[3] Kouzehgar M, Tamilselvam Y K, Heredia M V, et al. Self-reconfigurable façade-cleaning robot equipped with deep-learning-based crack detection based on convolutional neural networks. Automation in Construction, 2019, 108: 102959.

[4] Kim J. Autonomous robot vacuum system composed of a cleaner robot and a dust storage robot. Journal of the Franklin Institute, 2024: 106938.

[5] Palleja Cabre T, Tresanchez Ribes M, Teixido Cairol M, et al. Modeling floor-cleaning coverage performances of some domestic mobile robots in a reduced scenario. 2010.

[6] Wang D, Gao Y, Wei W, et al. Sliding mode observer-based model predictive tracking control for Mecanum-wheeled mobile robot. ISA transactions, 2024, 151: 51-61.

[7] Panda B, Dutta A. Design of a partially compliant crank rocker mechanism using ionic polymer metal composite for path generation. Materials & Design, 2010, 31(5): 2471-2477.

[8] Ma H, Song A, Li J, et al. Legged odometry based on fusion of leg kinematics and IMU information in a humanoid robot. Biomimetic Intelligence and Robotics, 2024: 100196.

[9] Chanekar P V, Ghosal A. Optimal synthesis of adjustable planar four-bar crank-rocker type mechanisms for approximate multi-path generation. Mechanism and Machine Theory, 2013, 69: 263-277.

[10] Sandor G N, Erdman A G. Mechanism design: analysis and synthesis. Prentice-Hall, 1984.

[11] Zhang J F, Xu Q Y. Research on stability of periodic elastic motion of a flexible four bar crank rocker mechanism. Journal of sound and vibration, 2004, 274(1-2): 39-51.

[12] Nathan W, Xianwen K, Suphi M E. Design of a train cleaning robot for the train carriage interior. Procedia CIRP, 2021, 100804-809.

[13] Zhao B, Yang J, Cao S, et al. Design of a vacuum-type PV module cleaning robot based on an auxiliary mobile frame. Solar Energy, 2024, 275: 112634.